

# Solving SU(3) Yang-Mills theory on the lattice: a calculation of selected gauge observables with gradient flow

---

Hans Mathias Mamen Vege

April 29, 2019

Supervisor: *Andrea Shindler*

Co-supervisor: *Morten Hjorth-Jensen*

University of Oslo

# Introduction

---

# Structure

- Quantum Chromodynamics(QCD).

- **QCD.** We will go through and explain what QCD as well as motivate its existence.

# Structure

- Quantum Chromodynamics(QCD).
- Lattice QCD.

1

- **QCD.** We will go through and explain what QCD as well as motivate its existence.
- **LQCD.** We will briefly show how one discretise the lattice and perform calculations on it.

# Structure

- Quantum Chromodynamics(QCD).
- Lattice QCD.
- Gradient flow.

1

- **QCD.** We will go through and explain what QCD as well as motivate its existence.
- **LQCD.** We will briefly show how one discretise the lattice and perform calculations on it.
- **Gradient flow.** We will quickly introduce gradient flow and explain its effects.

# Structure

- Quantum Chromodynamics(QCD).
- Lattice QCD.
- Gradient flow.
- Developing a code for solving  $SU(3)$  Yang-Mills theory.

1

- **QCD.** We will go through and explain what QCD as well as motivate its existence.
- **LQCD.** We will briefly show how one discretise the lattice and perform calculations on it.
- **Gradient flow.** We will quickly introduce gradient flow and explain its effects.
- **GLAC.** Will briefly present the code which we developed as well as some benchmarks. We will also present the Metropolis algorithm.

# Structure

- Quantum Chromodynamics(QCD).
- Lattice QCD.
- Gradient flow.
- Developing a code for solving  $SU(3)$  Yang-Mills theory.
- Results.

1

- **QCD.** We will go through and explain what QCD as well as motivate its existence.
- **LQCD.** We will briefly show how one discretise the lattice and perform calculations on it.
- **Gradient flow.** We will quickly introduce gradient flow and explain its effects.
- **GLAC.** Will briefly present the code which we developed as well as some benchmarks. We will also present the Metropolis algorithm.
- **Results.** We will present the results obtained from pure gauge calculations.

# Structure

- Quantum Chromodynamics(QCD).
- Lattice QCD.
- Gradient flow.
- Developing a code for solving  $SU(3)$  Yang-Mills theory.
- Results.

## Quantum Chromodynamics(QCD)

---

# QCD

- The standard model: Six quarks and eight gluons

- The standard model.

# QCD

- The standard model: Six quarks and eight gluons
- Asymptotic freedom

2

- The standard model.
- Asymptotic freedom.

- The standard model: Six quarks and eight gluons
- Asymptotic freedom
- Confinement

- The standard model.
- Asymptotic freedom.
- Confinement.

# QCD

- The standard model: Six quarks and eight gluons
- Asymptotic freedom
- Confinement
- Highly nonlinear due to gluon self-interactions

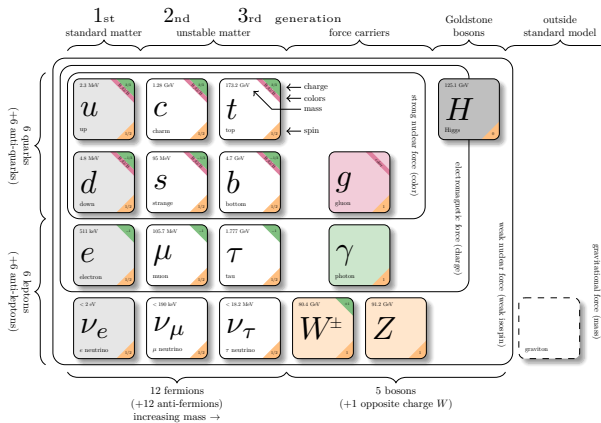
2

- The standard model.
- Asymptotic freedom.
- Confinement.
- Nonlinearity.

# QCD

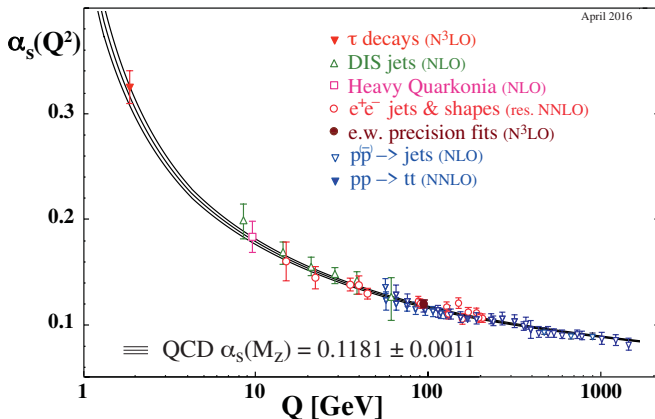
- The standard model: Six quarks and eight gluons
- Asymptotic freedom
- Confinement
- Highly nonlinear due to gluon self-interactions

# The Standard Model



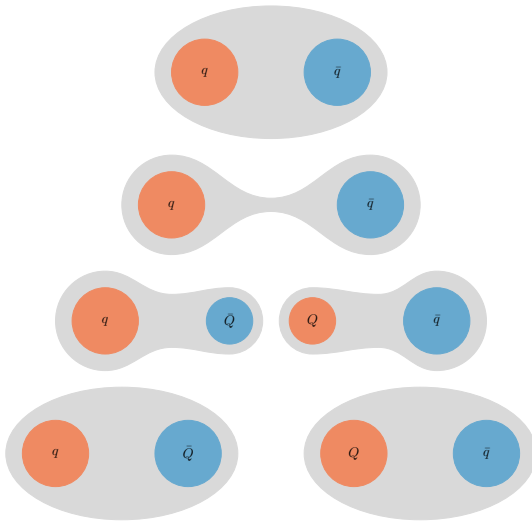
Consists of the innermost square of the six quarks and the gluons.

# Asymptotic freedom



- The coupling constant **decreases** as we **increase** the energy
- One of the experimental proofs of QCD along with triple  $\gamma$  decay and muon cross section ration  $R$ .

# Confinement



5

If we try to pull apart **two mesons**, more and more energy is required until we have enough energy to spontaneously create a **quark-antiquark pair**, forming thus **two new mesons**.

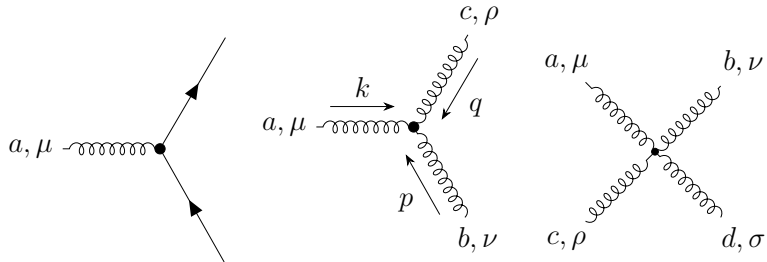
# The non-linearity of QCD

The QCD Lagrangian

$$\mathcal{L}_{\text{QCD}} = \sum_{f=1}^{N_f} \bar{\psi}^{(f)} \left( i \not{D} - m^{(f)} \right) \psi^{(f)} - \frac{1}{4} G_{\mu\nu}^a G^{a\mu\nu},$$

with action

$$S = \int d^4x \mathcal{L}_{\text{QCD}}. \quad (1)$$



# Topology in QCD

- Instantons

- **Instantons** are local minimums to the Yang-Mills action in Euclidean space.

# Topology in QCD

- Instantons
- Topological charge,  $Q$

7

- **Instantons** are local minimums to the Yang-Mills action in Euclidean space.
- Measuring **topological charge** is a measure of the *Winding number* of the gauge field.

# Topology in QCD

- Instantons
- Topological charge,  $Q$
- Winding number

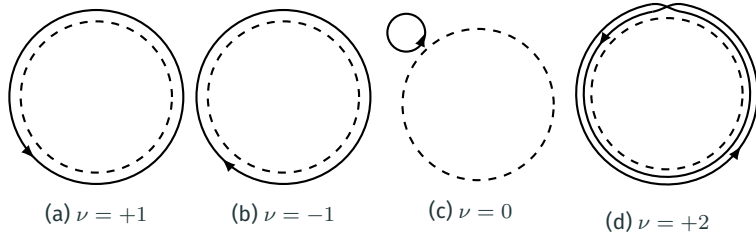


Figure 1: The figure is taken from Forkel [3, p. 32].

7

- **Instantons** are local minimums to the Yang-Mills action in Euclidean space.
- Measuring **topological charge** is a measure of the *Winding number* of the gauge field.
- An illustration of how one can view the winding number given a function  $f$  that parametrizes a path around a circle  $S^1$ . Given that it starts and ends at the same point, we have that the number of times it wraps around the circle gives us the winding number.

# Topology in QCD

- Instantons
- Topological charge,  $Q$
- Winding number

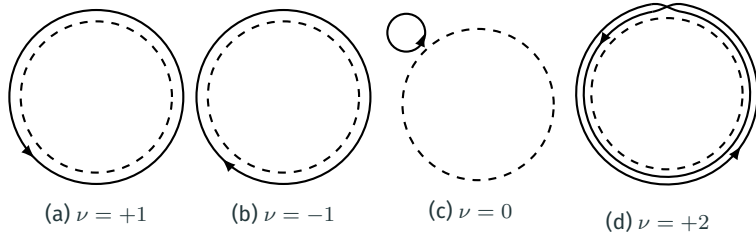


Figure 1: The figure is taken from Forkel [3, p. 32].

7

- **Instantons** are local minimums to the Yang-Mills action in Euclidean space.
- Measuring **topological charge** is a measure of the *Winding number* of the gauge field.
- An illustration of how one can view the winding number given a function  $f$  that parametrizes a path around a circle  $S^1$ . Given that it starts and ends at the same point, we have that the number of times it wraps around the circle gives us the winding number.

# The Witten-Veneziano relation

A formula connecting pure gauge theory and full QCD.

$$m_{\eta'}^2 = \frac{2N_f}{f_\pi^2} \chi_{\text{top}} \quad (2)$$

- Pion decay constant  $f_\pi = 0.130(5)/\sqrt{2}$  GeV.
- $\eta'$  meson mass  $m_{\eta'} = 0.95778(6)$  GeV.
- $\chi_{\text{top}}$  is the *topological susceptibility*.

8

- We use the experimental values for the pion decay constant and the  $\eta'$  mass.
- Allows us to estimate the number of flavors in our theory  $N_f$ .
- $\chi_{\text{top}}$  is the topological susceptibility, calculated from the expectation value of  $Q$ .

# Lattice Quantum Chromodynamics(LQCD)

---

# Discretizing spacetime

1. Divide spacetime into a cube of size  $N^3 \times N_T$ .

## Discretizing spacetime

1. Divide spacetime into a cube of size  $N^3 \times N_T$ .
2. Fermions live on the each *point* in the cube.

# Discretizing spacetime

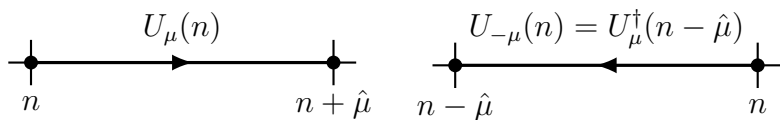
1. Divide spacetime into a cube of size  $N^3 \times N_T$ .
2. Fermions live on the each *point* in the cube.
3. The gauge fields live on the sites *in between* the points, and is called links.

# Links

A link

$$U_\mu(n) = \exp [iaA_\mu(n)],$$

connects one lattice site to another and is a  $SU(3)$  matrix.



where  $U_{-\mu}(n) = U_\mu(n - \hat{\mu})^\dagger$ .

- Defined from the gauge transporter.
- A link in the positive  $\hat{\mu}$  direction is shown in the figure to the left.
- A link in the negative  $\hat{\mu}$  direction is shown in the figure to the right.

# Gauge invariance on the lattice

Links gauge transform as

$$U_\mu(n) \rightarrow U'_\mu(n) = \Omega(n) U_\mu(n) \Omega(n + \hat{\mu})^\dagger,$$
$$U_{-\mu}(n) \rightarrow U'_{-\mu}(n) = \Omega(n) U_\mu(n - \hat{\mu})^\dagger \Omega(n - \hat{\mu})^\dagger.$$

# Gauge invariance on the lattice

Links gauge transform as

$$U_\mu(n) \rightarrow U'_\mu(n) = \Omega(n) U_\mu(n) \Omega(n + \hat{\mu})^\dagger,$$
$$U_{-\mu}(n) \rightarrow U'_{-\mu}(n) = \Omega(n) U_\mu(n - \hat{\mu})^\dagger \Omega(n - \hat{\mu})^\dagger.$$

Two main types of gauge invariant objects,

# Gauge invariance on the lattice

Links gauge transform as

$$U_\mu(n) \rightarrow U'_\mu(n) = \Omega(n) U_\mu(n) \Omega(n + \hat{\mu})^\dagger,$$
$$U_{-\mu}(n) \rightarrow U'_{-\mu}(n) = \Omega(n) U_\mu(n - \hat{\mu})^\dagger \Omega(n - \hat{\mu})^\dagger.$$

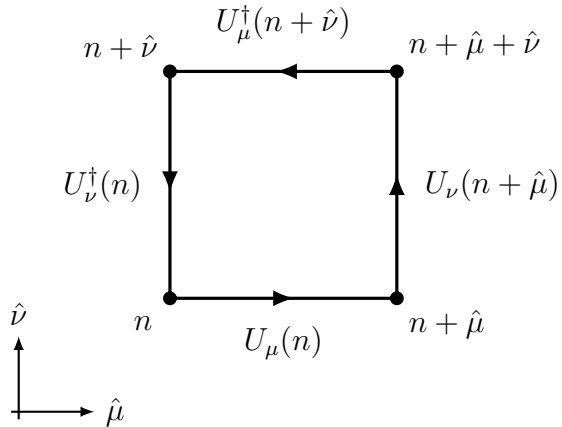
Two main types of gauge invariant objects,

- Fully connected gauge invariant objects.
- Objects with fermions  $\psi, \bar{\psi}$  as end points.

# The plaquette

The simplest gauge invariant object,

$$\begin{aligned} P_{\mu\nu}(n) &= U_\mu(n) U_\nu(n + \hat{\mu}) U_{-\mu}(n + \hat{\mu} + \hat{\nu}) U_{-\nu}(n + \hat{\nu}) \\ &= U_\mu(n) U_\nu(n + \hat{\mu}) U_\mu(n + \hat{\nu})^\dagger U_\nu(n)^\dagger, \end{aligned}$$



# The Wilson gauge action

The Wilson gauge action is given as

$$S_G[U] = \frac{\beta}{3} \sum_{n \in \Lambda} \sum_{\mu < \nu} \text{Re} \operatorname{tr} [1 - P_{\mu\nu}(n)], \quad (3)$$

with  $\beta = 6/g_S^2$ .

- Using the definition of the link we saw earlier, we can reproduce the continuum action up to a discretization error of  $\mathcal{O}(a^2)$ .

# Developing a code for solving SU(3) Yang-Mills theory on the lattice

---

# The numerical challenge in lattice QCD

A lattice configuration consists of SU(3) matrices,

14

- The SU(3) matrices are  $3 \times 3$  matrices of nine complex numbers or 18 real numbers.
- This leads to an absolute **requirement of efficiency**, both in **calculations** and in **input/output**.
- When returning to what ensembles of configurations we generated this will be evident.

# The numerical challenge in lattice QCD

A lattice configuration consists of SU(3) matrices,

$$\underbrace{N^3}_{\text{Spatial}} \times \underbrace{N_T}_{\text{Temporal}} \times \underbrace{4}_{\text{Links}} \times \underbrace{9}_{\text{SU(3) matrix}} \times \underbrace{2}_{\mathbb{C}\text{-numbers}} = 72N^3N_T,$$

- The SU(3) matrices are  $3 \times 3$  matrices of nine complex numbers or 18 real numbers.
- This leads to an absolute **requirement of efficiency**, both in **calculations** and in **input/output**.
- When returning to what ensembles of configurations we generated this will be evident.

# The numerical challenge in lattice QCD

A lattice configuration consists of  $SU(3)$  matrices,

$$\underbrace{N^3}_{\text{Spatial}} \times \underbrace{N_T}_{\text{Temporal}} \times \underbrace{4}_{\text{Links}} \times \underbrace{9}_{\text{\text{SU}(3) matrix}} \times \underbrace{2}_{\mathbb{C}\text{-numbers}} = 72N^3N_T,$$

$\rightarrow 8 \times 72N^3N_T$  bytes.

- The  $SU(3)$  matrices are  $3 \times 3$  matrices of nine complex numbers or 18 real numbers.
- This leads to an absolute **requirement of efficiency**, both in **calculations** and in **input/output**.
- When returning to what ensembles of configurations we generated this will be evident.

# The path integral I

$$\langle O \rangle = \frac{1}{Z} \int \mathcal{D}U O[\psi, \bar{\psi}, U] e^{-S_G[U] - S_F[\psi, \bar{\psi}, U]}.$$

with

$$Z = \int \mathcal{D}U \mathcal{D}\bar{\psi} \mathcal{D}\psi e^{-S_G[U] - S_F[\psi, \bar{\psi}, U]}.$$

# The path integral I

$$\langle O \rangle = \frac{1}{Z} \int \mathcal{D}U O[U] e^{-S_G[U]}.$$

with

$$Z = \int \mathcal{D}U e^{-S_G[U]}.$$

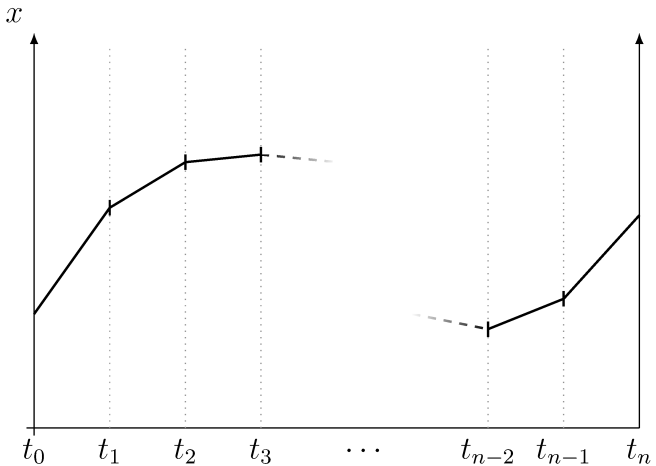
# The path integral I

$$\langle O \rangle = \frac{1}{Z} \int \mathcal{D}U O[U] e^{-S_G[U]}.$$

with

$$Z = \int \mathcal{D}U e^{-S_G[U]}.$$

## The path integral II



16

An example of the discretized path integral, going from time  $t_0$  to  $t_{N_T}$ , where the end points is taken to be equal,  $x_0 = x_{N_T}$ . We integrate over all of space at each time  $t_i$  finding the most likely position at a given time.

## How to measure

The observable becomes an average over the  $N_{\text{MC}}$  gauge configurations.

$$\langle O \rangle = \lim_{N_{\text{MC}} \rightarrow \infty} \frac{1}{N_{\text{MC}}} \sum_i^{N_{\text{MC}}} O[U_i]$$

We now need to generate configurations...

- We perform an average of the created configurations.

# The Metropolis algorithm

**repeat**

Randomly generate a candidate state  $j$  with probability  $T_{i \rightarrow j}$ .

Calculate  $A_{i \rightarrow j}$  which saw on previous slide.

Generate random number  $u \in [0, 1]$ .

**if**  $u \leq A_{i \rightarrow j}$  **then**

    Accept new state  $j$ .

**else if**  $u > A_{i \rightarrow j}$  **then**

    Reject new state  $j$  and retain the old state  $i$ .

**end if**

**until**  $N_{MC}$  samples are generated.

- Generated state  $j$  is a gauge configuration.
- Algorithm of choice when sampling gauge configurations.
- For generating  $N_{MC}$  Monte Carlo samples.

# The Metropolis algorithm on the lattice

A parameter  $\epsilon_{\text{rnd}}$  controls the spread of the candidate matrices.

1. Initialize lattice with SU(3) matrices close to unity(*hot start*) or at unity(*cold start*).
2. Thermalize with  $N_{\text{therm}}$  sweeps.
3. Generate  $N_{\text{MC}}$  samples,
  - i Perform  $N_{\text{corr}}$  correlation updates.
  - ii At each update, perform  $N_{\text{up}}$  single link update for every lattice link.
  - iii Store configuration and/or apply gradient flow and sample observables on it.

- We use **periodic boundary conditions** for all calculations.
- $N_{\text{MC}}$  is how many configurations we will generate.
- $N_{\text{up}}$  is how many single link updates we will perform.
- $N_{\text{corr}}$  is how many full sweeps we shall perform in between each sampling. Needed in order to reduce the autocorrelation between the configurations.

# Parallelization

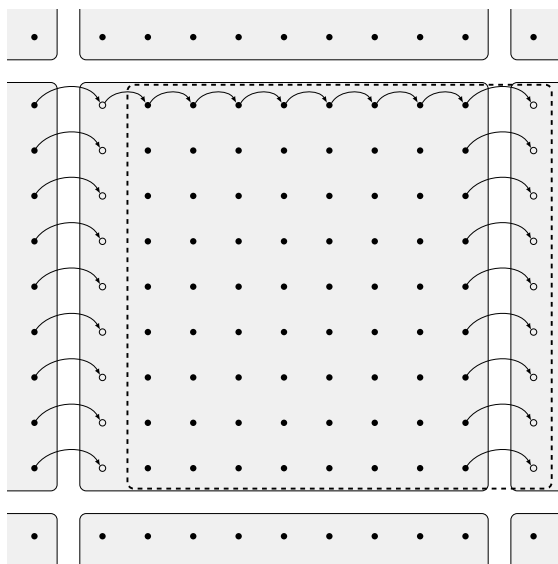
Two methods used:

- Single link sharing used in the Metropolis algorithm.
- *shifts* used in gradient flow and observable sampling

20

- Tested out **halos**, but turned out to be problematic when generating.
- We parallelized using MPI.

# Shifts



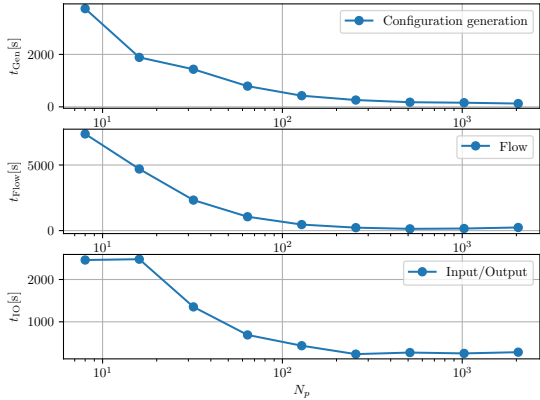
21

- An illustration of the lattice shift.
- The links  $U_\nu$  of the lattice are copied over to a temporary lattice shifted in direction  $\hat{\mu}$ .
- The face that is shifted over to an adjacent sub-lattice is shared through a non-blocking MPI call, while we copy the links to the temporary lattice.
- Allows for a simplified syntax close to that of the equations we are working with.
- Don't have to write out any loops over the lattice positions.

# Scaling

We checked three types of scaling,

- Strong scaling: *fixed problem* and a *variable  $N_p$  cores*

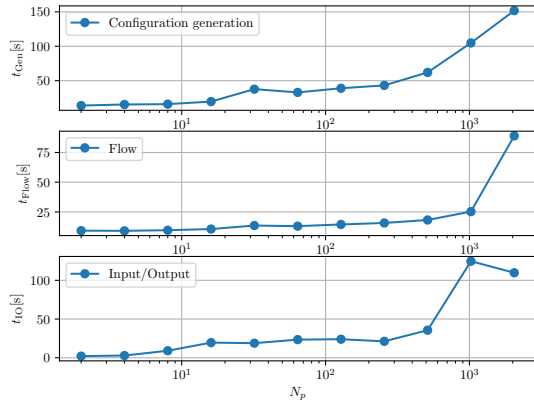


- Strong scaling

# Scaling

We checked three types of scaling,

- **Strong scaling:** *fixed problem* and a variable  $N_p$  cores
- **Weak scaling:** *fixed problem per processor* and a variable  $N_p$  cores.



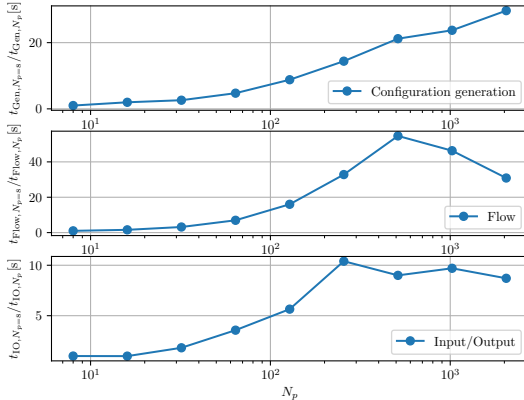
22

- Strong scaling
- Weak scaling

# Scaling

We checked three types of scaling,

- **Strong scaling:** *fixed problem* and a *variable  $N_p$  cores*
- **Weak scaling:** *fixed problem per processor* and a *variable  $N_p$  cores.*
- **Speedup:** defined as  $S(p) = \frac{t_{N_p=0}}{t_{N_p}}$ .



22

- Strong scaling
- Weak scaling
- The speedup of the configuration generation, flowing, and IO. The speedup is calculated by dividing the run time of each  $N_p$  run, with the run time of the run with the least number of processors,  $N_p = 8$ .

We appear to have a plateau around 512 cores.

We checked three types of scaling,

- **Strong scaling:** *fixed problem and a variable  $N_p$  cores*
- **Weak scaling:** *fixed problem per processor and a variable  $N_p$  cores.*
- **Speedup:** defined as  $S(p) = \frac{t_{N_p,0}}{t_{N_p}}$ .

22

- Strong scaling
- Weak scaling
- The speedup of the configuration generation, flowing, and IO. The speedup is calculated by dividing the run time of each  $N_p$  run, with the run time of the run with the least number of processors,  $N_p = 8$ .

We appear to have a plateau around 512 cores.

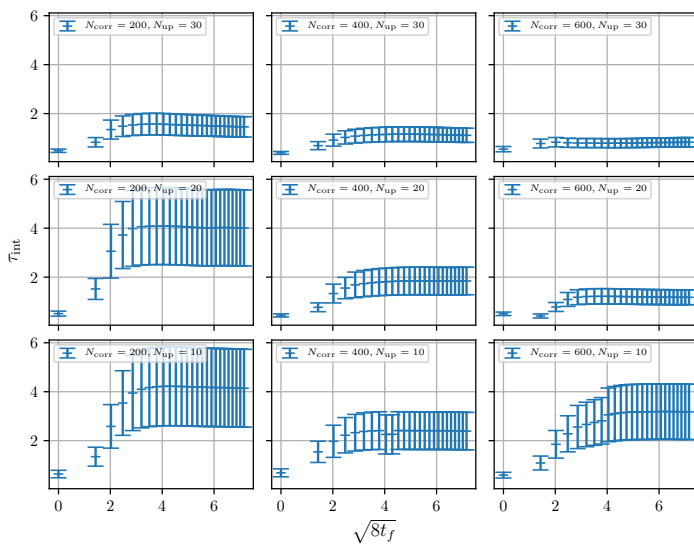
# Optimizing the gauge configuration generation

Generated 200 configurations for a lattice of size  $N^3 \times N_T = 16^3 \times 32$  and  $\beta = 6.0$ , for combinations of  $N_{\text{corr}} \in [200, 400, 600]$  and  $N_{\text{up}} \in [10, 20, 30]$ .

23

- We run for different values for  $N_{\text{up}}$  and  $N_{\text{corr}}$  to see what gives optimizes **computational cost** and **autocorrelation**.
- The integrated autocorrelation time for topological charge  $\langle Q \rangle$  for a lattice of size  $N = 16$  and  $N_T = 32$  with  $\beta = 6.0$  for combinations of  $N_{\text{corr}} \in [200, 400, 600]$  and  $N_{\text{up}} \in [10, 20, 30]$ , plotted against flow time  $\sqrt{8t_f}$ .

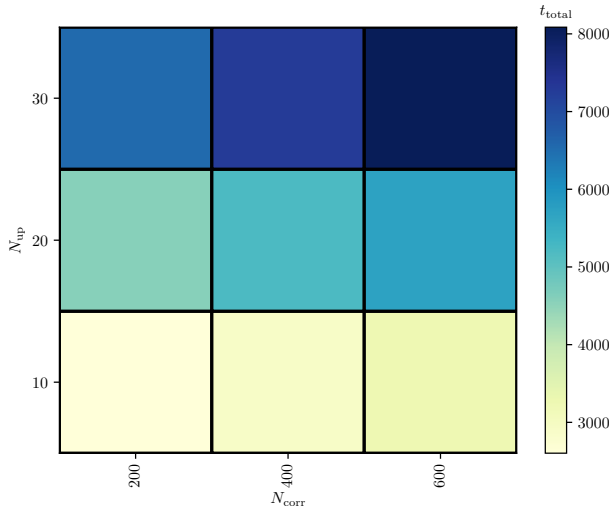
# Optimizing the gauge configuration generation



23

- We run for different values for  $N_{\text{up}}$  and  $N_{\text{corr}}$  to see what gives optimizes **computational cost** and **autocorrelation**.
- The time taking to generate 200 configurations and flowing them  $N_{\text{flow}} = 250$  flow steps for a lattice of size  $N = 16$  and  $N_T = 32$ , with  $\beta = 6.0$  for combinations of  $N_{\text{corr}} \in [200, 400, 600]$  and  $N_{\text{up}} \in [10, 20, 30]$ .

# Optimizing the gauge configuration generation



23

- We run for different values for  $N_{\text{up}}$  and  $N_{\text{corr}}$  to see what gives optimizes **computational cost** and **autocorrelation**.
- The time taking to generate 200 configurations and flowing them  $N_{\text{flow}} = 250$  flow steps for a lattice of size  $N = 16$  and  $N_T = 32$ , with  $\beta = 6.0$  for combinations of  $N_{\text{corr}} \in [200, 400, 600]$  and  $N_{\text{up}} \in [10, 20, 30]$ .

## Gradient flow

---

## The flow equation

The flow of the SU(3) gauge fields are denoted by  $B_\mu(x, t_f)$  which are Lie algebra valued gauge fields,

$$\frac{d}{dt_f} B_\mu(x, t_f) = D_\nu G_{\nu \mu}(x, t_f), \quad (4)$$

- The flow equation in the continuum is defined by this differential equation.

## The flow equation

The flow of the SU(3) gauge fields are denoted by  $B_\mu(x, t_f)$  which are Lie algebra valued gauge fields,

$$\frac{d}{dt_f} B_\mu(x, t_f) = D_\nu G_{\nu \mu}(x, t_f), \quad (4)$$

$$D_\mu = \partial_\mu + [B_\mu(x, t_f), \cdot], \quad (5)$$

- The flow equation in the continuum is defined by this differential equation.
- With the covariant derivative given by following, with the  $\cdot$  being the derivative with respect to flow time.

## The flow equation

The flow of the SU(3) gauge fields are denoted by  $B_\mu(x, t_f)$  which are Lie algebra valued gauge fields,

$$\frac{d}{dt_f} B_\mu(x, t_f) = D_\nu G_{\nu \mu}(x, t_f), \quad (4)$$

$$D_\mu = \partial_\mu + [B_\mu(x, t_f), \cdot], \quad (5)$$

$$G_{\mu\nu}(x, t_f) = \partial_\mu B_\nu(x, t_f) - \partial_\nu B_\mu(x, t_f) - i[B_\mu(x, t_f), B_\nu(x, t_f)], \quad (6)$$

- The flow equation in the continuum is defined by this differential equation.
- With the covariant derivative given by following, with the  $\cdot$  being the derivative with respect to flow time.
- The field strength tensor of the flown fields is given in the regular format.

## The flow equation

The flow of the SU(3) gauge fields are denoted by  $B_\mu(x, t_f)$  which are Lie algebra valued gauge fields,

$$\frac{d}{dt_f} B_\mu(x, t_f) = D_\nu G_{\nu \mu}(x, t_f), \quad (4)$$

$$D_\mu = \partial_\mu + [B_\mu(x, t_f), \cdot], \quad (5)$$

$$G_{\mu\nu}(x, t_f) = \partial_\mu B_\nu(x, t_f) - \partial_\nu B_\mu(x, t_f) - i[B_\mu(x, t_f), B_\nu(x, t_f)], \quad (6)$$

with the initial conditions being the fundamental gauge field,

$$B_\mu(x, t_f)|_{t_f=0} = A_\mu(x).$$

- The flow equation in the continuum is defined by this differential equation.
- With the covariant derivative given by following, with the  $\cdot$  being the derivative with respect to flow time.
- The field strength tensor of the flown fields is given in the regular format.
- The initial condition is the un-flowed gauge field,  $A_\mu$ .

# The flow equation

The flow of the SU(3) gauge fields are denoted by  $B_\mu(x, t_f)$  which are Lie algebra valued gauge fields,

$$\frac{d}{dt_f} B_\mu(x, t_f) = D_\nu G_{\nu \mu}(x, t_f), \quad (4)$$

$$D_\mu = \partial_\mu + [B_\mu(x, t_f), \cdot], \quad (5)$$

$$G_{\mu\nu}(x, t_f) = \partial_\mu B_\nu(x, t_f) - \partial_\nu B_\mu(x, t_f) - i[B_\mu(x, t_f), B_\nu(x, t_f)], \quad (6)$$

with the initial conditions being the fundamental gauge field,

$$B_\mu(x, t_f)|_{t_f=0} = A_\mu(x).$$

A bad approximation: *the diffusion equation*,

$$\frac{\partial}{\partial t_f} B_\mu(x, t_f) \approx \partial^2 B_\mu(x, t_f)$$

24

- The flow equation in the continuum is defined by this differential equation.
- With the covariant derivative given by following, with the  $\cdot$  being the derivative with respect to flow time.
- The field strength tensor of the flown fields is given in the regular format.
- The initial condition is the un-flowed gauge field,  $A_\mu$ .
- Bad approx.: diffusion equation.

# The flow equation

The flow of the SU(3) gauge fields are denoted by  $B_\mu(x, t_f)$  which are Lie algebra valued gauge fields,

$$\frac{d}{dt_f} B_\mu(x, t_f) = D_\nu G_{\nu \mu}(x, t_f), \quad (4)$$

$$D_\mu = \partial_\mu + [B_\mu(x, t_f), \cdot], \quad (5)$$

$$G_{\mu\nu}(x, t_f) = \partial_\mu B_\nu(x, t_f) - \partial_\nu B_\mu(x, t_f) - i[B_\mu(x, t_f), B_\nu(x, t_f)], \quad (6)$$

with the initial conditions being the fundamental gauge field,

$$B_\mu(x, t_f)|_{t_f=0} = A_\mu(x).$$

A bad approximation: *the diffusion equation*,

$$\frac{\partial}{\partial t_f} B_\mu(x, t_f) \approx \partial^2 B_\mu(x, t_f)$$

The smearing radius increases as  $\sqrt{8t_f}$ .

24

- The flow equation in the continuum is defined by this differential equation.
- With the covariant derivative given by following, with the  $\cdot$  being the derivative with respect to flow time.
- The field strength tensor of the flown fields is given in the regular format.
- The initial condition is the un-flowed gauge field,  $A_\mu$ .
- Bad approx.: diffusion equation.
- Topological charge preserved and is more pronounced.
- Renormalizes the topological charge at non-zero flow time.

# The flow equation

The flow of the SU(3) gauge fields are denoted by  $B_\mu(x, t_f)$  which are Lie algebra valued gauge fields,

$$\frac{d}{dt_f} B_\mu(x, t_f) = D_\nu G_{\nu \mu}(x, t_f), \quad (4)$$

$$D_\mu = \partial_\mu + [B_\mu(x, t_f), \cdot], \quad (5)$$

$$G_{\mu\nu}(x, t_f) = \partial_\mu B_\nu(x, t_f) - \partial_\nu B_\mu(x, t_f) - i[B_\mu(x, t_f), B_\nu(x, t_f)], \quad (6)$$

with the initial conditions being the fundamental gauge field,

$$B_\mu(x, t_f)|_{t_f=0} = A_\mu(x).$$

A bad approximation: *the diffusion equation*,

$$\frac{\partial}{\partial t_f} B_\mu(x, t_f) \approx \partial^2 B_\mu(x, t_f)$$

The smearing radius increases as  $\sqrt{8t_f}$ .

24

- The flow equation in the continuum is defined by this differential equation.
- With the covariant derivative given by following, with the  $\cdot$  being the derivative with respect to flow time.
- The field strength tensor of the flown fields is given in the regular format.
- The initial condition is the un-flowed gauge field,  $A_\mu$ .
- Bad approx.: diffusion equation.
- Topological charge preserved and is more pronounced.
- Renormalizes the topological charge at non-zero flow time.

## Gradient flow on the lattice

$$\dot{V}_{tf}(x, \mu) = -g_S^2 \left\{ \partial_{x,\mu} S_G[V_{tf}] \right\} V_{tf}(x, \mu),$$

25

- On the lattice, the flow equation takes the shape in terms of the link variables.

## Gradient flow on the lattice

$$\dot{V}_{tf}(x, \mu) = -g_S^2 \left\{ \partial_{x,\mu} S_G[V_{tf}] \right\} V_{tf}(x, \mu),$$

with initial condition,

$$V_{tf}(x, \mu)|_{t_f=0} = U(x, \mu)$$

- On the lattice, the flow equation takes the shape in terms of the link variables.
- Initial conditions similar to the continuum case.

## Gradient flow on the lattice

$$\dot{V}_{tf}(x, \mu) = -g_S^2 \left\{ \partial_{x,\mu} S_G[V_{tf}] \right\} V_{tf}(x, \mu),$$

with initial condition,

$$V_{tf}(x, \mu)|_{t_f=0} = U(x, \mu)$$

Note: need to find the action derivative  $S_G[V_{tf}]$ .

- On the lattice, the flow equation takes the shape in terms of the link variables.
- Initial conditions similar to the continuum case.
- The action derivative is also needed, but that is a minor task we will not cover here.

## Gradient flow on the lattice

$$\dot{V}_{tf}(x, \mu) = -g_S^2 \left\{ \partial_{x,\mu} S_G[V_{tf}] \right\} V_{tf}(x, \mu),$$

with initial condition,

$$V_{tf}(x, \mu)|_{t_f=0} = U(x, \mu)$$

Note: need to find the action derivative  $S_G[V_{tf}]$ .

- On the lattice, the flow equation takes the shape in terms of the link variables.
- Initial conditions similar to the continuum case.
- The action derivative is also needed, but that is a minor task we will not cover here.

# Solving gradient flow with Runge-Kutta 3

With

$$\dot{V}_{tf} = -g_S^2 \left\{ \partial_{x,\mu} S_G[V_{tf}] \right\} V_{tf} = Z(V_{tf}) V_{tf},$$

- We rewrite the equations slightly,

# Solving gradient flow with Runge-Kutta 3

With

$$\dot{V}_{tf} = -g_S^2 \left\{ \partial_{x,\mu} S_G[V_{tf}] \right\} V_{tf} = Z(V_{tf}) V_{tf},$$

we get

$$W_0 = V_{tf},$$

$$W_1 = \exp \left[ \frac{1}{4} Z_0 \right] W_0,$$

$$W_2 = \exp \left[ \frac{8}{9} Z_1 - \frac{17}{36} Z_0 \right] W_1,$$

$$V_{tf+\epsilon_f} = \exp \left[ \frac{3}{4} Z_2 - \frac{8}{9} Z_1 + \frac{17}{36} Z_0 \right] W_2,$$

with coefficients from Lüscher [4].

- We rewrite the equations slightly,
- and use a structure preserving integrator with coefficients from Lüscher [4].

# Solving gradient flow with Runge-Kutta 3

With

$$\dot{V}_{tf} = -g_S^2 \left\{ \partial_{x,\mu} S_G[V_{tf}] \right\} V_{tf} = Z(V_{tf}) V_{tf},$$

we get

$$W_0 = V_{tf},$$

$$W_1 = \exp \left[ \frac{1}{4} Z_0 \right] W_0,$$

$$W_2 = \exp \left[ \frac{8}{9} Z_1 - \frac{17}{36} Z_0 \right] W_1,$$

$$V_{tf+\epsilon_f} = \exp \left[ \frac{3}{4} Z_2 - \frac{8}{9} Z_1 + \frac{17}{36} Z_0 \right] W_2,$$

with coefficients from Lüscher [4].

26

- We rewrite the equations slightly,
- and use a structure preserving integrator with coefficients from Lüscher [4].
- We control the accuracy of this integrator by  $\epsilon_f$ .

# Solving gradient flow with Runge-Kutta 3

With

$$\dot{V}_{tf} = -g_S^2 \left\{ \partial_{x,\mu} S_G[V_{tf}] \right\} V_{tf} = Z(V_{tf}) V_{tf},$$

we get

$$W_0 = V_{tf},$$

$$W_1 = \exp \left[ \frac{1}{4} Z_0 \right] W_0,$$

$$W_2 = \exp \left[ \frac{8}{9} Z_1 - \frac{17}{36} Z_0 \right] W_1,$$

$$V_{tf+\epsilon_f} = \exp \left[ \frac{3}{4} Z_2 - \frac{8}{9} Z_1 + \frac{17}{36} Z_0 \right] W_2,$$

with coefficients from Lüscher [4].

26

- We rewrite the equations slightly,
- and use a structure preserving integrator with coefficients from Lüscher [4].
- We control the accuracy of this integrator by  $\epsilon_f$ .

## Verifying the integration

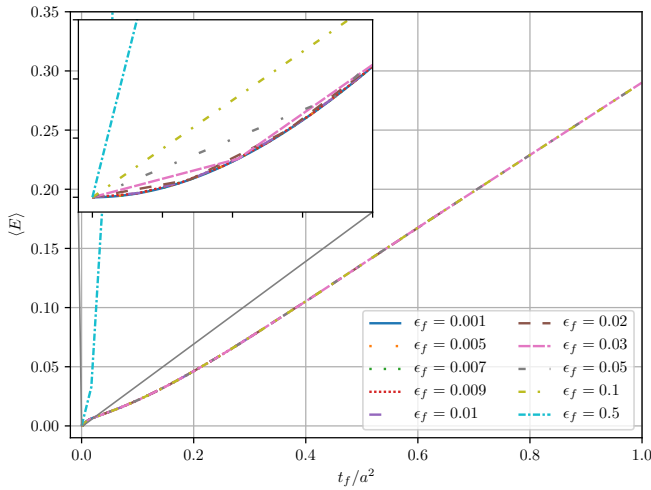
Testing the integrator for different integration steps  $\epsilon_f$ .

$\epsilon_f$	0.001	0.005	0.007	0.009	0.01	0.02	0.03	0.05	0.1	0.5
--------------	-------	-------	-------	-------	------	------	------	------	-----	-----

- The values we will test the integrator against.

## Verifying the integration

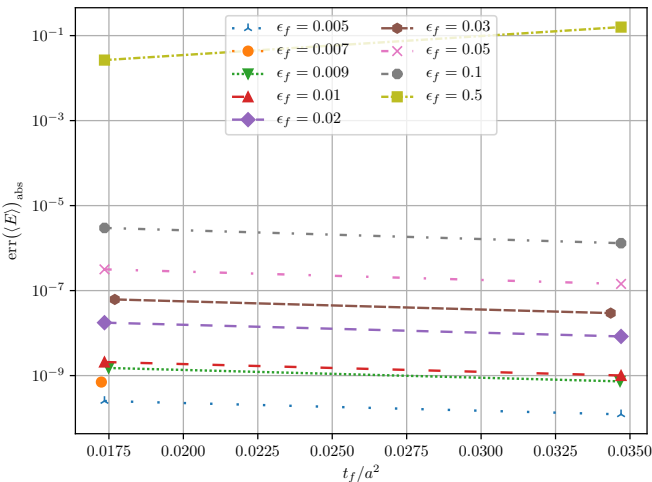
Lattice size  $N^3 \times N_T = 24^3 \times 48$  with  $\beta = 6.0$ .



- The values we will test the integrator against.
- The energy flowed for different the different  $\epsilon_f$  values.

## Verifying the integration

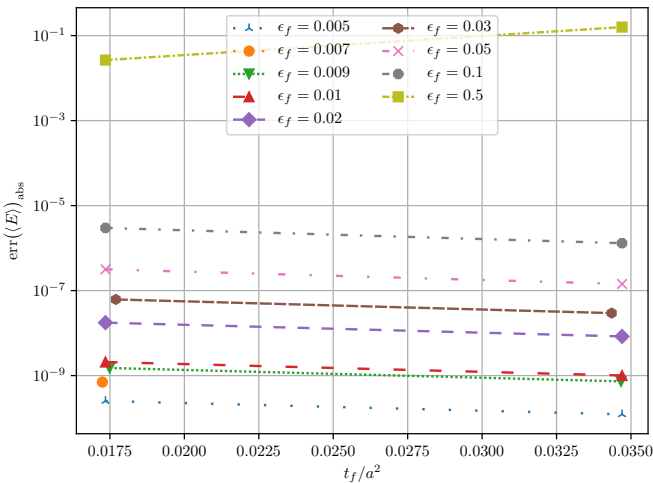
The absolute difference between the smallest flow time  $\epsilon_f = 0.001$  and those shown previously.



- The values we will test the integrator against.
- The energy flowed for different the different  $\epsilon_f$  values.
- The absolute difference between the smallest flow time  $\epsilon_f = 0.001$  and those listed in previous table.
- The reason for **only having two points** is due to the fact that we are **only comparing points** that are **close to each other in flow time**. If we were to have more points, we would have to double the number of flow time steps for the smallest lattices.

## Verifying the integration

The absolute difference between the smallest flow time  $\epsilon_f = 0.001$  and those shown previously.

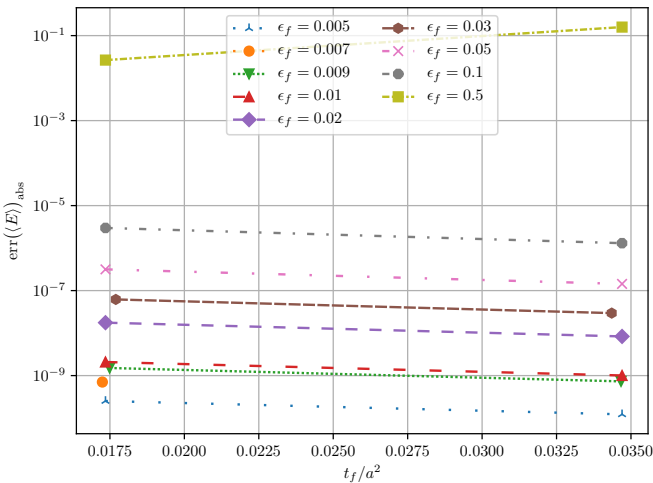


27

- The values we will test the integrator against.
- The energy flowed for different the different  $\epsilon_f$  values.
- The absolute difference between the smallest flow time  $\epsilon_f = 0.001$  and those listed in previous table.
- The reason for **only having two points** is due to the fact that we are **only comparing points** that are **close to each other in flow time**. If we were to have more points, we would have to double the number of flow time steps for the smallest lattices.
- An **example** of the flowing, can be seen by observing the **energy evolving over flow time**.

## Verifying the integration

The absolute difference between the smallest flow time  $\epsilon_f = 0.001$  and those shown previously.



27

- The values we will test the integrator against.
- The energy flowed for different the different  $\epsilon_f$  values.
- The absolute difference between the smallest flow time  $\epsilon_f = 0.001$  and those listed in previous table.
- The reason for **only having two points** is due to the fact that we are **only comparing points** that are **close to each other in flow time**. If we were to have more points, we would have to double the number of flow time steps for the smallest lattices.
- An **example** of the flowing, can be seen by observing the **energy evolving over flow time**.

## Results

---

# Ensembles

Ensemble	$\beta$	$N$	$N_T$	$N_{\text{cfg}}$	$\epsilon_{\text{flow}}$	Config. size[GB]
$A$	6.0	24	48	1000	0.01	0.356
$B$	6.1	28	56	1000	0.01	0.659
$C$	6.2	32	64	2000	0.01	1.125
$D_1$	6.45	32	32	1000	0.02	0.563
$D_2$	6.45	48	96	250	0.02	5.695

- We use  $N_{\text{corr}} = 1600$  for  $\beta = 6.45$  ensembles,  $N_{\text{corr}} = 600$  for the rest.

- The main ensembles made for this thesis.
- Every configuration was flown with  $N_{\text{flow}} = 1000$  flow steps.
- We should also mention that we generated a few additional ensembles for investigating other aspects of the topological charge.

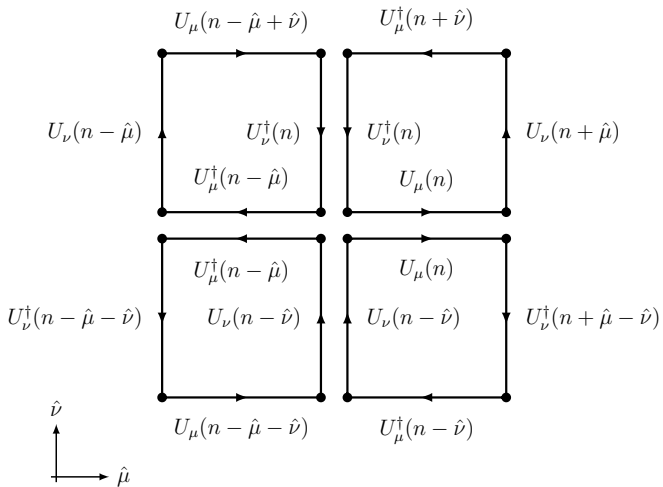
# Ensembles

Ensemble	$\beta$	$N$	$N_T$	$N_{\text{cfg}}$	$\epsilon_{\text{flow}}$	Config. size[GB]
$A$	6.0	24	48	1000	0.01	0.356
$B$	6.1	28	56	1000	0.01	0.659
$C$	6.2	32	64	2000	0.01	1.125
$D_1$	6.45	32	32	1000	0.02	0.563
$D_2$	6.45	48	96	250	0.02	5.695

- We use  $N_{\text{corr}} = 1600$  for  $\beta = 6.45$  ensembles,  $N_{\text{corr}} = 600$  for the rest.
- $N_{\text{up}} = 30$ .

- The main ensembles made for this thesis.
- Every configuration was flown with  $N_{\text{flow}} = 1000$  flow steps.
- We should also mention that we generated a few additional ensembles for investigating other aspects of the topological charge.

# The clover field strength definition



- We will use the clover field strength definition in gauge observables.

## Energy definition

$$E = \frac{a^4}{2|\Lambda|} \sum_{n \in \Lambda} \sum_{\mu, \nu} (F_{\mu\nu}^{\text{clov}}(n))^2$$

30

- We can use this definition to set a scale.

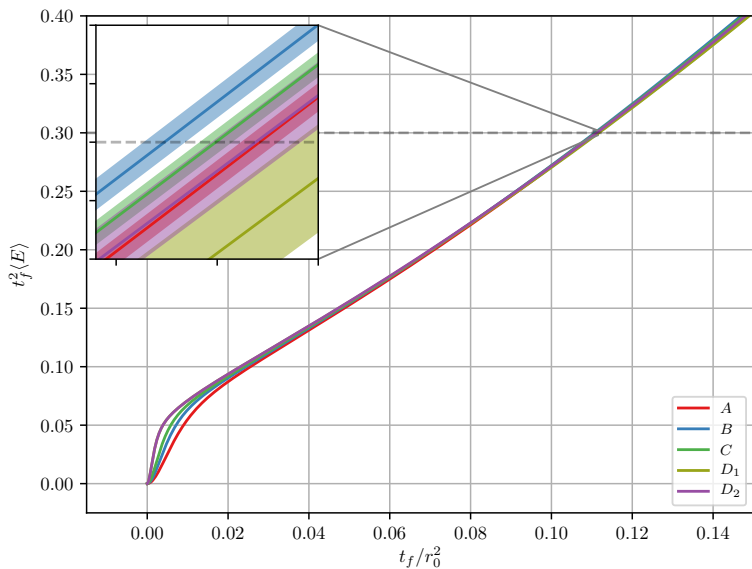
## Energy definition

$$E = \frac{a^4}{2|\Lambda|} \sum_{n \in \Lambda} \sum_{\mu, \nu} (F_{\mu\nu}^{\text{clov}}(n))^2$$

We can use this definition to set a scale  $t_0$ ,

$$\left\{ t_f^2 \langle E(t) \rangle \right\}_{t_f=t_0} = 0.3.$$

- We can use this definition to set a scale.



## Scale setting $t_0$

Ensemble	$L/a$	$L$ [fm]	$a$ [fm]
$A$	24	2.235(9)	0.0931(4)
$B$	28	2.214(10)	0.0791(3)
$C$	32	2.17(1)	0.0679(3)
$D_1$	32	1.530(9)	0.0478(3)
$D_2$	48	2.29(1)	0.0478(3)

## Scale setting $t_0$

Ensemble	$t_0[\text{fm}^2]$	$t_0/a^2$	$t_0/r_0^2$
$A$	0.02780(2)	3.20(3)	0.11121(9)
$B$	0.02769(2)	4.43(4)	0.11075(10)
$C$	0.02775(2)	6.01(6)	0.11099(8)
$D_1$	0.02779(5)	12.2(1)	0.1112(2)
$D_2$	0.02794(9)	12.2(1)	0.1117(3)

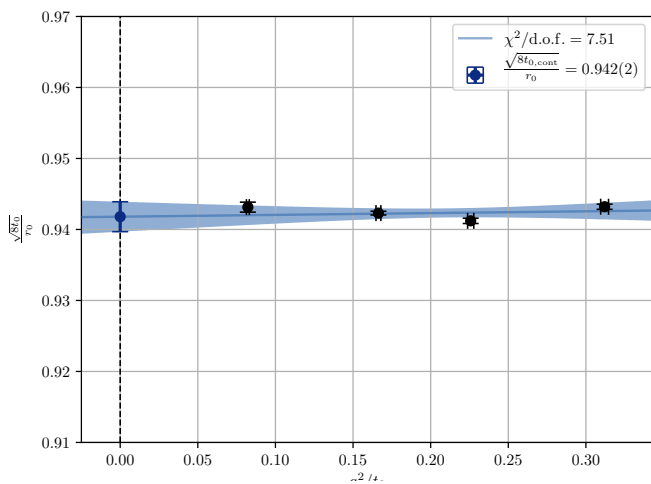
- Extrapolation results for  $t_0$ , where we retrieved the exact point of intersection between  $t_f^2 \langle E \rangle$  and 0.3 using  $N_{\text{bs}} = 500$  bootstrap fits. Extrapolating to the continuum gives us  $t_{0,\text{cont}}/r_0^2 = 0.11087(50)$ .

## Scale setting $t_0$

Ensemble	$t_0[\text{fm}^2]$	$t_0/a^2$	$t_0/r_0^2$
$A$	0.02780(2)	3.20(3)	0.11121(9)
$B$	0.02769(2)	4.43(4)	0.11075(10)
$C$	0.02775(2)	6.01(6)	0.11099(8)
$D_1$	0.02779(5)	12.2(1)	0.1112(2)
$D_2$	0.02794(9)	12.2(1)	0.1117(3)

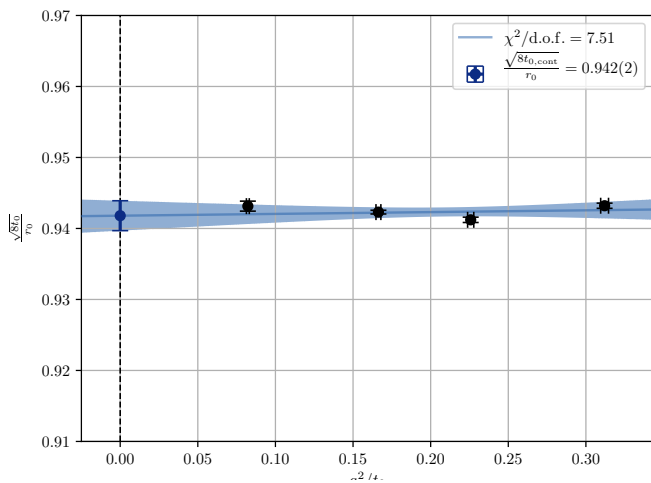
- Extrapolation results for  $t_0$ , where we retrieved the exact point of intersection between  $t_f^2 \langle E \rangle$  and 0.3 using  $N_{\text{bs}} = 500$  bootstrap fits. Extrapolating to the continuum gives us  $t_{0,\text{cont}}/r_0^2 = 0.11087(50)$ .

## Scale setting $t_0$



- The continuum extrapolation  $a \rightarrow 0$  for  $t_0$  of the four ensembles  $A$ ,  $B$ ,  $C$ , and  $D_2$ .

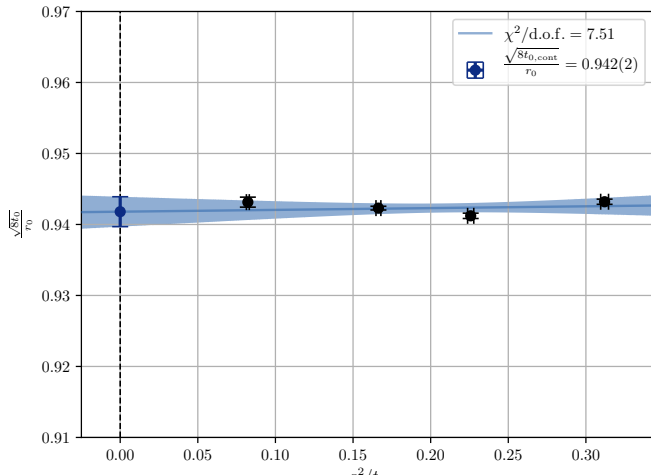
## Scale setting $t_0$



Continuum extrapolation using ensembles  $A$ ,  $B$ ,  $C$ , and  $D_2$  gives  $t_{0,\text{cont}}/r_0^2 = 0.11087(50)$ .

- The continuum extrapolation  $a \rightarrow 0$  for  $t_0$  of the four ensembles  $A$ ,  $B$ ,  $C$ , and  $D_2$ .
- $r_0 = 0.5$  fm.

## Scale setting $t_0$



Continuum extrapolation using ensembles  $A$ ,  $B$ ,  $C$ , and  $D_2$  gives  $t_{0,\text{cont}}/r_0^2 = 0.11087(50)$ . This matches the values retrieved by Lüscher [4].

- The continuum extrapolation  $a \rightarrow 0$  for  $t_0$  of the four ensembles  $A$ ,  $B$ ,  $C$ , and  $D_2$ .
- $r_0 = 0.5$  fm.

## Scale setting $t_0$

Extrapolations for different ensemble-combinations

Ensembles	$\frac{t_0, \text{cont}}{r_0^2}$	$\chi^2/\text{d.o.f}$
$A, B, C, D_2$	0.11087(50)	7.51
$B, C, D_2$	0.1115(3)	0.41
$A, B, C, D_1$	0.1119(6)	0.88

## Scale setting $w_0$

Can also set a scale using the derivative which offers more granularity for small flow times,

$$W(t)|_{t=w_0^2} = 0.3,$$
$$W(t) \equiv t_f \frac{d}{dt_f} \{ t_f^2 \langle E \rangle \}.$$

## Scale setting $w_0$

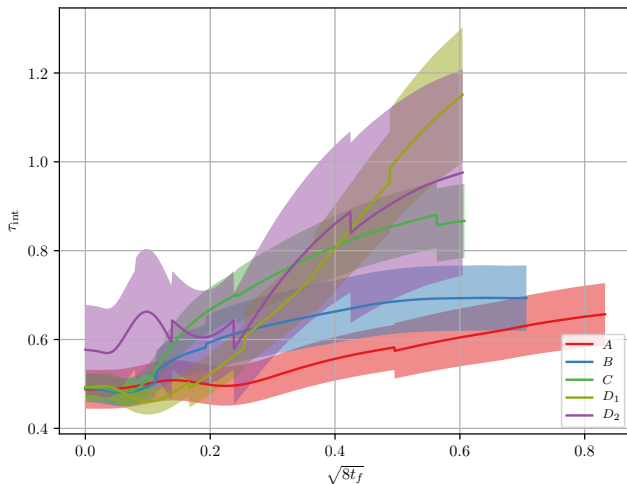
Ensembles	$w_{0\text{cont}}[\text{fm}]$	$\chi^2/\text{d.o.f}$
$A, B, C, D_2$	0.1695(5)	7.12
$B, C, D_2$	0.1702(3)	0.53
$A, B, C, D_1$	0.1706(6)	0.86

## Scale setting $w_0$

Ensembles	$w_{0\text{cont}}[\text{fm}]$	$\chi^2/\text{d.o.f}$
$A, B, C, D_2$	0.1695(5)	7.12
$B, C, D_2$	0.1702(3)	0.53
$A, B, C, D_1$	0.1706(6)	0.86

Comparable to Borsanyi et al. [1] which included dynamical fermions, with  $w_{0,\text{cont}} = 0.1755(18)(04)$  fm.

## Autocorrelation in the energy



The autocorrelation of the energy. A value of  $\tau_{\text{int}} = 0.5$  indicates that we have zero autocorrelation.

## Topological charge definition

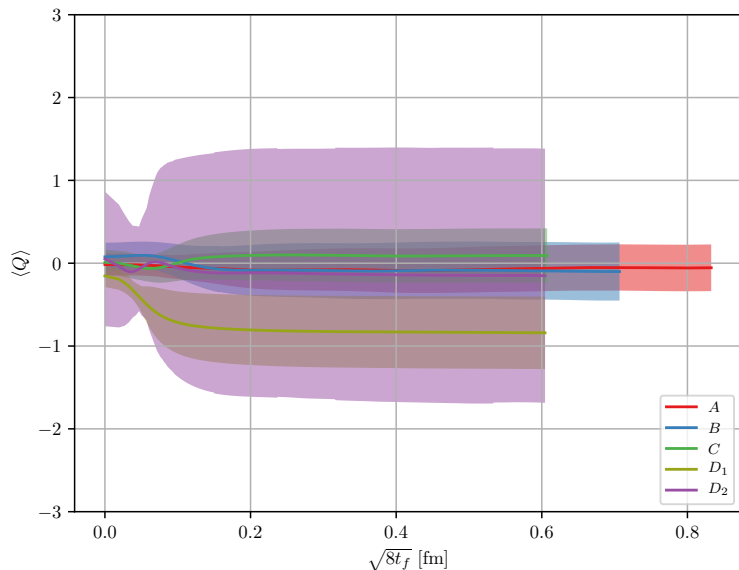
$$Q = a^4 \sum_{n \in \Lambda} q(n),$$

with the charge density given by

$$q(n) = \frac{1}{32\pi^2} \epsilon_{\mu\nu\rho\sigma} \text{tr} [F_{\mu\nu}(n) F_{\rho\sigma}(n)].$$

- We will use the clover field strength definition.
- Symmetries will allow us to reduce the effective number of clovers need to calculate from 24 to 6.

# Topological charge



38

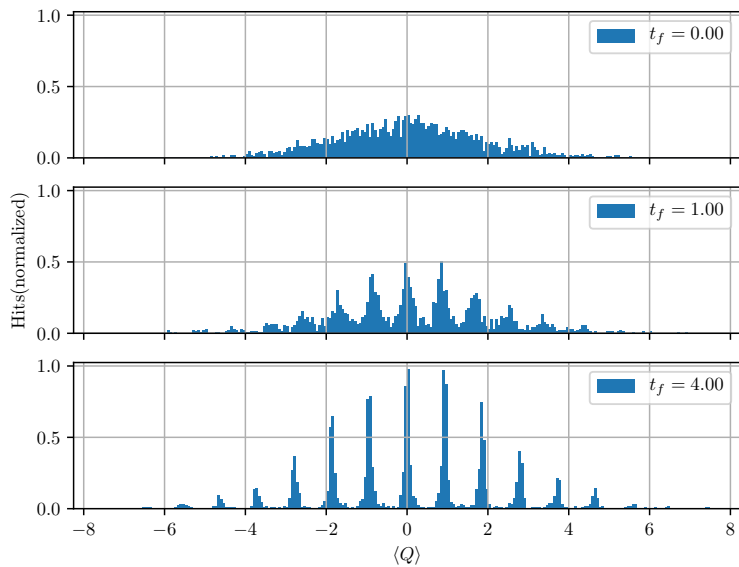
- Topological charge  $Q$  as evolved in flow time for the five main ensembles.
- Bootstrapped data with  $N_{\text{bs}} = 500$  bootstrap samples.
- Corrected for autocorrelations with  $\sigma = \sqrt{2\tau_{\text{int}}}\sigma_0$ .

## Additional ensembles

Ensemble	$N$	$N_T$	$N_{\text{cfg}}$	$N_{\text{corr}}$	$N_{\text{up}}$	$a$ [fm]	$L$ [fm]
$E$	8	16	8135	600	30	0.0931(4)	0.745(3)
$F$	12	24	1341	200	20	0.0931(4)	1.118(5)
$G$	16	32	2000	400	20	0.0790(3)	1.265(6)

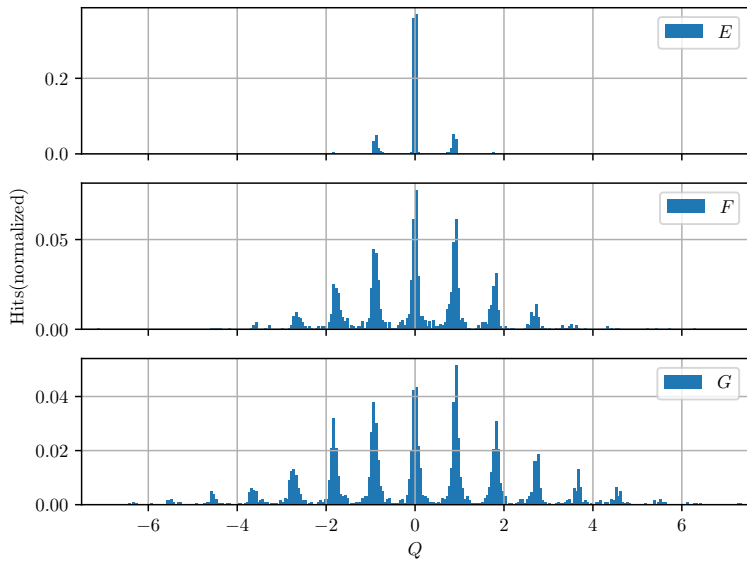
- Additional ensembles made in order to illuminate additional aspects of the topological charge.
- Supporting ensembles made on Smaug. All ensembles were flown  $N_{\text{flow}} = 1000$  steps with  $\epsilon_{\text{flow}} = 0.01$ .

# Topological charge distribution



Histograms for the topological charge for ensemble  $G$  with a lattice of size  $N^3 \times N_T = 16^3 \times 32$  with  $\beta = 6.1$ , taken at different flow times  $t_f/a^2 = 0.0, 1.0, 4.0$  fm.

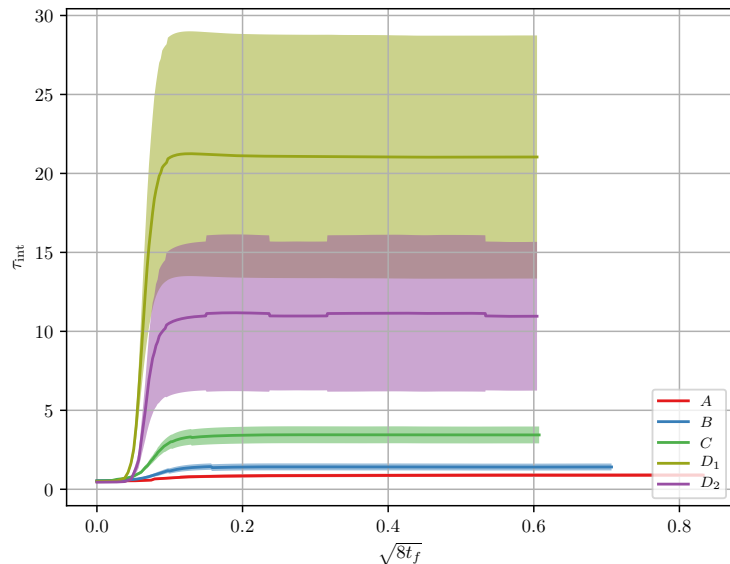
# Topological charge distribution in flow time



41

Histograms of topological charge for the supporting ensembles seen at  $t_f/a^2 = 0.25$  fm.

# Topological charge autocorrelation

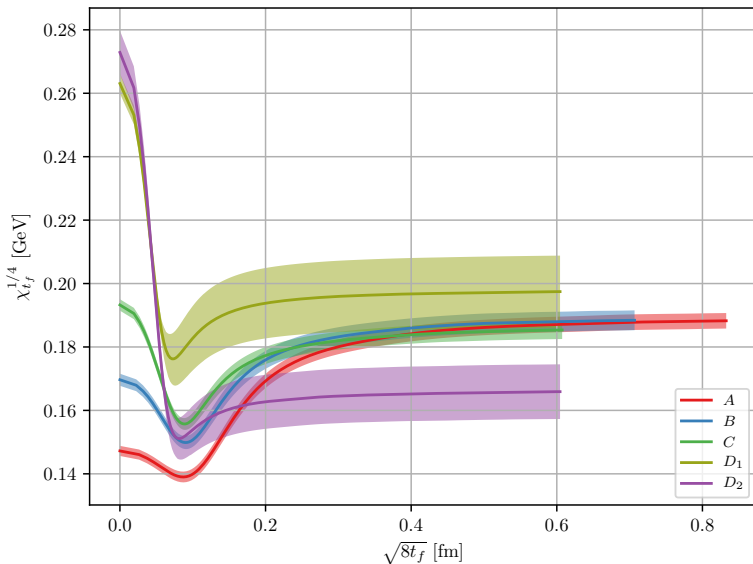


The integrated autocorrelation  $\tau_{\text{int}}$  for topological charge for the five main ensembles.

## Topological susceptibility

$$\chi_{\text{top}}^{1/4} = \frac{1}{V^{1/4}} \langle Q^2 \rangle^{1/4}$$

# Topological susceptibility



- The topological susceptibility  $\chi_{tf}^{1/4}$  of the main ensembles.
- Bootstrapped  $N_{\text{bs}} = 500$  times.
- Corrected for autocorrelations with  $\sigma = \sqrt{2\tau_{\text{int}}}\sigma_0$ .

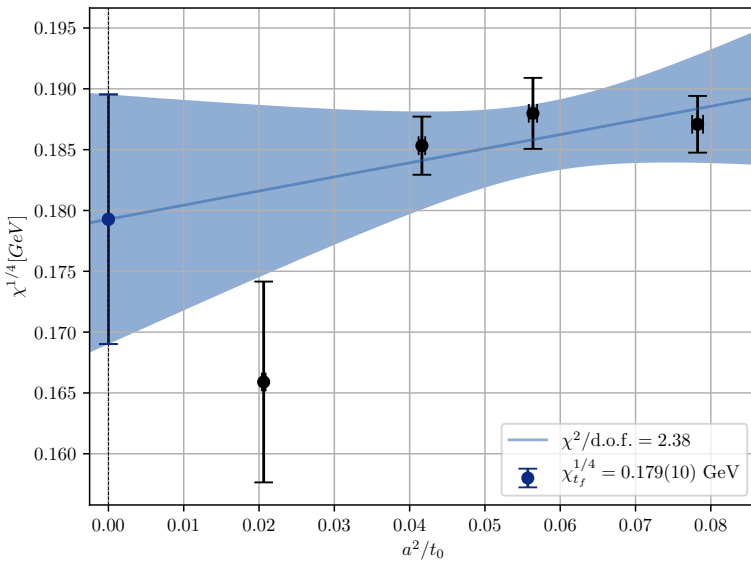
# Topological susceptibility continuum extrapolation

Ensemble	$\chi_{tf}^{1/4}$ [GeV]	$\chi_{tf}^{1/4}$ [GeV], corrected	$\sqrt{2\tau_{int}}$
<i>A</i>	0.1877(23)	0.1877(24)	1.028(46)
<i>B</i>	0.1880(21)	0.1880(29)	1.346(81)
<i>C</i>	0.1853(14)	0.1853(24)	1.762(104)
<i>D</i> <sub>1</sub>	0.1971(22)	0.1971(101)	4.523(675)
<i>D</i> <sub>2</sub>	0.1656(33)	0.1656(86)	2.624(441)

Error corrected for autocorrelations with  $\sigma = \sqrt{2\tau_{int}}\sigma_0$ .

The topological susceptibility for the main ensembles together with the correction factor from the integrated autocorrelation time. The second column have not had its results corrected by  $\sqrt{2\tau_{int}}$ . None of the results have been analyzed with bootstrapping.

# Topological susceptibility continuum extrapolation



46

- A continuum extrapolation of the topological susceptibility  $\chi_{tf}^{1/4}$  for the main ensembles excluding the  $D_1$  ensemble.
- The points for  $\chi_{tf}^{1/4}$  is taken at  $\sqrt{8t_{f,0}} = 0.6$  fm.

# Topological susceptibility continuum extrapolation

Ensembles	$\chi_{tf}^{1/4} (\langle Q^2 \rangle) [\text{GeV}]$	$N_f$	$\chi^2/\text{d.o.f}$
$A, B, C, D_2$	0.179(10)	3.75(29)	2.38
$A, B, C, D_1$	0.186(6)	3.21(25)	0.83
$B, C, D_1$	0.187(24)	3.18(24)	1.63
$B, C, D_2$	0.166(24)	5.06(39)	2.05
$A, B, C$	0.184(6)	3.37(26)	0.33

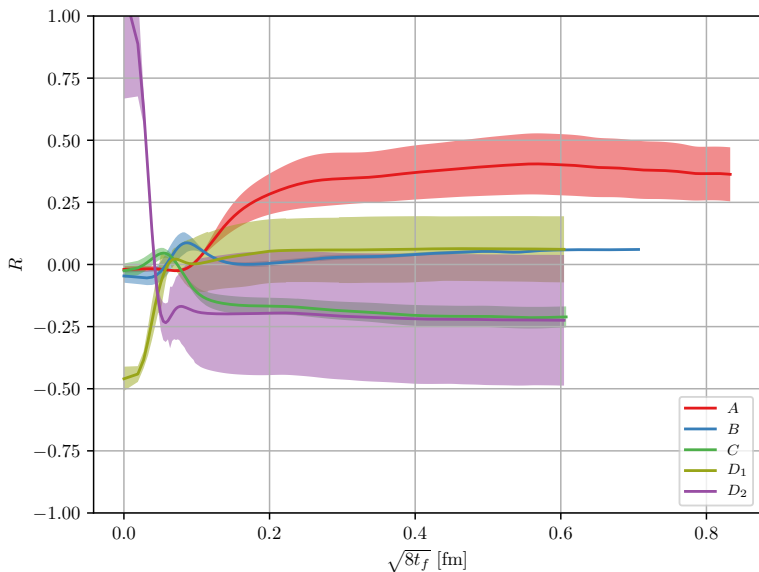
## The fourth cumulant

$$\langle Q^4 \rangle_c = \frac{1}{V^2} \left( \langle Q^4 \rangle - 3 \langle Q^2 \rangle^2 \right).$$

From this, we can also measure the ratio  $R$ ,

$$R = \frac{\langle Q^4 \rangle_c}{\frac{1}{V} \langle Q^2 \rangle} = \frac{1}{V} \frac{\langle Q^4 \rangle - 3 \langle Q^2 \rangle^2}{\langle Q^2 \rangle},$$

# The fourth cumulant



- The fourth cumulant ratio  $R = \langle Q^4 \rangle_C / \langle Q^2 \rangle$ .
- The results were analyzed using  $N_{\text{bs}} = 500$  bootstrap samples, with the error corrected for by  $\sqrt{2\tau_{\text{int}}}$ .

# The fourth cumulant at reference flow times

Ensemble	$L/a$	$t_0/a^2$	$\langle Q^2 \rangle$	$\langle Q^4 \rangle$	$\langle Q^4 \rangle_C$
$A$	2.24	3.20(3)	0.78(4)	2.13(27)	0.282(67)
$B$	2.21	4.43(4)	0.81(5)	1.98(23)	0.036(11)
$C$	2.17	6.01(6)	0.77(4)	1.6(2)	-0.174(40)
$D_1$	1.53	12.2(1)	1.00(20)	3.01(1.07)	0.03(12)
$D_2$	2.29	12.2(1)	0.497(100)	0.64(20)	-0.103(95)

The fourth cumulant is taken at their individual reference scales seen in the third column. The data were analyzed with using a bootstrap analysis of  $N_{bs} = 500$  samples, with error corrected by the integrated autocorrelation,  $\sqrt{2\tau_{int}}$ .

# Comparing fourth cumulant

Ensemble	$\beta$	$L/a$	$L$ [fm]	$a$ [fm]	$t_0/a^2$	$t_0/r_0^2$	
$F_1$	5.96	16	1.632	0.102	2.7887(2)	0.1113(9)	1 440
$B_2$	6.05	14	1.218	0.087	3.7960(12)	0.1114(9)	144
$\tilde{D}_2$		17	1.479		3.7825(8)	0.1110(9)	
$B_3$	6.13	16	1.232	0.077	4.8855(15)	0.1113(10)	144
$\tilde{D}_3$		19	1.463		4.8722(11)	0.1110(10)	
$B_4$	6.21	18	1.224	0.068	6.2191(20)	0.1115(11)	144
$\tilde{D}_4$		21	1.428		6.1957(14)	0.1111(11)	

- Parameters of the ensembles presented by Cè et al. [2]. The first column is the ensemble name from the article. The letter indicates the volume, while the subindex indicates the  $\beta$  value. Ensembles of similar letters keep approximately the same length  $L$ .

# Comparing fourth cumulant

Ensemble	$\langle Q^2 \rangle_{\text{normed}}$	$\langle Q^4 \rangle_{\text{normed}}$	$\langle Q^4 \rangle_{C,\text{normed}}$	$R_{\text{normed}}$
$F_1$	0.728(1)	1.608(4)	0.016(1)	0.022(1)
$B_2$	0.772(3)	1.873(19)	0.085(4)	0.110(5)
$\tilde{D}_2$	0.770(3)	1.817(17)	0.037(4)	0.048(5)
$B_3$	0.760(3)	1.805(17)	0.074(3)	0.097(4)
$\tilde{D}_3$	0.769(3)	1.801(14)	0.027(1)	0.035(1)
$B_4$	0.776(3)	1.874(18)	0.069(3)	0.089(4)
$\tilde{D}_4$	0.785(3)	1.891(17)	0.040(4)	0.052(5)

- Parameters of the ensembles presented by Cè et al. [2]. The first column is the ensemble name from the article. The letter indicates the volume, while the subindex indicates the  $\beta$  value. Ensembles of similar letters keep approximately the same length  $L$ .
- Results as presented by Cè et al. [2], normalized by the lattice volume.

# Comparing fourth cumulant

Article	Thesis	Ratio( $\langle Q^2 \rangle$ )	Ratio( $\langle Q^4 \rangle$ )	Ratio( $\langle Q^4 \rangle_C$ )	Ratio( $R$ )
$F_1$	$A$	1.08(6)	1.34(18)	19.03(5.81)	17.64(4.48)
$B_2$	$A$	1.02(5)	1.15(15)	3.60(1.09)	3.54(90)
	$B$	1.04(6)	1.06(11)	0.480(74)	0.46(4)
$\tilde{D}_2$	$A$	1.02(5)	1.19(15)	8.31(1.99)	8.15(1.56)
	$B$	1.05(6)	1.10(12)	1.1(1)	1.06(3)
$B_3$	$B$	1.06(6)	1.10(12)	0.550(86)	0.52(5)
$\tilde{D}_3$	$B$	1.05(6)	1.11(12)	1.51(23)	1.4(1)
$B_4$	$C$	0.99(5)	0.86(8)	-2.32(46)	-2.35(59)
$\tilde{D}_4$	$C$	0.98(5)	0.85(8)	-3.95(96)	-4.05(1.19)

- Parameters of the ensembles presented by Cè et al. [2]. The first column is the ensemble name from the article. The letter indicates the volume, while the subindex indicates the  $\beta$  value. Ensembles of similar letters keep approximately the same length  $L$ .
- Results as presented by Cè et al. [2], normalized by the lattice volume.
- A comparison between the results obtained in this thesis on the fourth cumulant, and by those similar in volume form Cè et al. [2]. *Ratio* indicates that we are dividing our results by the ones in previous table.

## Comparing fourth cumulant

51

- Parameters of the ensembles presented by Cè et al. [2]. The first column is the ensemble name from the article. The letter indicates the volume, while the subindex indicates the  $\beta$  value. Ensembles of similar letters keep approximately the same length  $L$ .
- Results as presented by Cè et al. [2], normalized by the lattice volume.
- A comparison between the results obtained in this thesis on the fourth cumulant, and by those similar in volume form Cè et al. [2]. *Ratio* indicates that we are dividing our results by the ones in previous table.

# The topological charge correlator

# The effective glueball mass

## Conclusion

---



Questions?

- [1] S. Borsanyi, S. Durr, Z. Fodor, C. Hoelbling, S. D. Katz, S. Krieg, T. Kurth, L. Lellouch, T. Lippert, C. McNeile, and K. K. Szabo. High-precision scale setting in lattice QCD. *Journal of High Energy Physics*, 2012(9), September 2012. ISSN 1029-8479. doi: 10.1007/JHEP09(2012)010. URL <http://arxiv.org/abs/1203.4469>. arXiv: 1203.4469.
- [2] Marco Cè, Cristian Consonni, Georg P. Engel, and Leonardo Giusti. Non-Gaussianities in the topological charge distribution of the SU(3) Yang–Mills theory. *Physical Review D*, 92(7), October 2015. ISSN 1550-7998, 1550-2368. doi: 10.1103/PhysRevD.92.074502. URL <http://arxiv.org/abs/1506.06052>. arXiv: 1506.06052.
- [3] Hilmar Forkel. A Primer on Instantons in QCD. *arXiv:hep-ph/0009136*, September 2000. URL <http://arxiv.org/abs/hep-ph/0009136>. arXiv: hep-ph/0009136.
- [4] Martin Lüscher. Properties and uses of the Wilson flow in lattice QCD. *Journal of High Energy Physics*, 2010(8), August 2010. ISSN 1029-8479. doi: 10.1007/JHEP08(2010)071. URL <http://arxiv.org/abs/1006.4518>. arXiv: 1006.4518.